THE JOURNAL OF PHYSICAL CHEMISTRY B
A JOURNAL OF THE AMERICAN CHEMICAL SOCIETY

pubs.acs.org/JPCB

Article

Kinetic and Calorimetric Fragility of Chalcogenide Glass-Forming Liquids: Role of Shear vs Enthalpy Relaxation

Yiqing Xia, Bing Yuan, Ozgur Gulbiten, Bruce Aitken, and Sabyasachi Sen*

Cite This: https://dx.doi.org/10.1021/acs.jpcb.0c11278

Read Online

ACCESS | Metrics & More | Article Recommendations

ABSTRACT: The kinetic and calorimetric fragility indices m of binary As−Se and Se−Te chalcogenide liquids with a wide range of fragility are determined using a combination of parallel plate rheometry, beam bending viscometry, and conventional differential scanning calorimetry (DSC). It is shown that both sets of measurements lead to consistent m values only if the validity of the assumptions often implicit in the methodology for the estimation of m are considered. These assumptions are (i) the glass transition temperature T_g corresponds to a viscosity of $\sim 10^{12}$ Pa s and (ii) enthalpy and shear relaxation time scales τ_{en} and τ_{shear} are comparable near T_g. Both assumptions are shown to be untenable for highly fragile liquids, for which modulated DSC studies demonstrate that $\tau_{en} \gg \tau_{shear}$ near T_g. In these cases, the above-mentioned assumptions are shown to lead to consistently higher values for the kinetic fragility compared to its calorimetric counterpart.

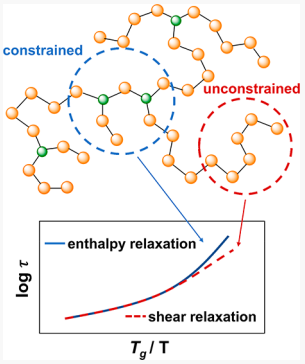

1. INTRODUCTION

The temperature dependence of the viscosity $\eta(T)$ is perhaps the most important physical characteristic of glass-forming liquids that controls their viability for various manufacturing methods.[1−4] The two key parameters used in the modeling of this temperature dependence are the glass transition temperature T_g, defined here as the temperature where the average structural relaxation time of the glass-forming liquid is on the order of ∼100 s, and the steepness of the slope of $\eta(T)$ at $T \approx T_g$. The latter parameter is formally expressed in the form of the fragility index m, which is given by the relation:[5−8]

$$m = \left.\frac{\mathrm{d}\log_{10}\eta}{\mathrm{d}\left(\frac{T_g}{T}\right)}\right|_{T_g=T} \quad (1)$$

Although the viscosity of a glass-forming liquid can increase by ≥12 orders of magnitude upon supercooling from its melting point to T_g, Angell has shown that η for a large variety of these liquids follows a rather predictable pattern when plotted as a function of the scaled temperature T_g/T and consequently, following eq 1, m serves as a key parameter for their classification.[6,7] Glass-forming liquids with relatively low and high values of m were termed by Angell as "strong" and "fragile", respectively, and m can range between ∼20 and 100 for inorganic liquids.[8] The temperature dependence of η becomes increasingly non-Arrhenius, i.e., the activation energy becomes increasingly temperature dependent with increasing m.

In spite of the simplicity of the mathematical form of eq 1, direct experimental determination of $\eta(T)$ at $T \approx T_g$ remains rather challenging due to the long equilibration times involved with the relaxation of the sample. Additionally, some glasses tend to crystallize during these long equilibration times upon heating above T_g. On the other hand, a large body of literature exists on a variety of glass-forming liquids that seems to suggest that $\eta \approx 10^{12}$ Pa s at $T \approx T_g$. Therefore, it has become a common practice in the literature to assign this viscosity to the calorimetrically determined T_g, combine this data point with the viscosity data measured at $T > T_g$ over a wide temperature and viscosity range, and fit these data with empirical or phenomenological equations to obtain m. However, it has recently been shown that relatively large inconsistencies can exist between the m values determined for a liquid, depending on the viscosity/temperature range that is considered for fitting and on which equation is used to fit the $\eta(T)$ data, especially for fragile liquids.[9,10] A case in point is liquid selenium (Se), where m was shown to span a range of ∼68 to 95 (Figure 1) depending on the temperature range of the $\eta(T)$ data used and whether such data were fitted to the Vogel−Fulcher−Tammann (VFT) relation, the Mauro−Yue−Ellison−Gupta−Allen (MYEGA) equation or the Avramov-Milchev (AM)

Received: December 18, 2020
Revised: January 29, 2021

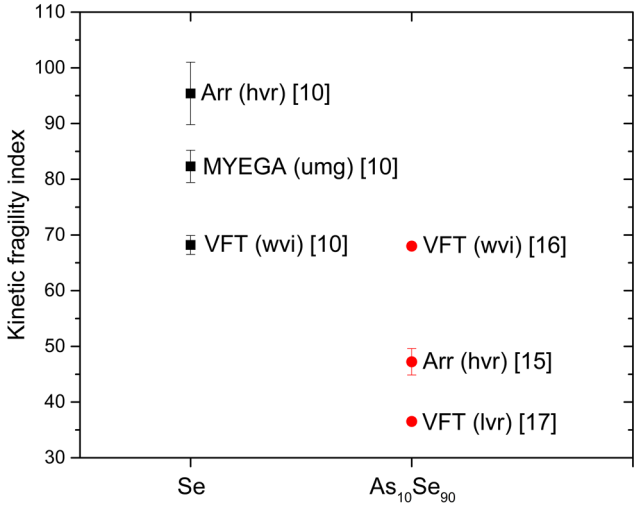

Figure 1. Kinetic fragility index of Se (black squares) and $As_{10}Se_{90}$ (red circles) determined from viscosity data reported in the literature.[10,15−17] Viscosity data fitting models (Arr: Arrhenius; MYEGA: Mauro-Yue- Ellison-Gupta-Allan; VFT: Vogel−Fulcher−Tammann) and the viscosity regions (umg: undercooled melt and glass region; hvr: high viscosity ($\sim 10^{10.5}$−$10^{12.5}$ Pa s) region; wvi: whole viscosity interval; lvr: heavily weighted low viscosity ($\sim 10^{3}$−10^{5} Pa s) region) used for fitting are denoted alongside the corresponding data points.

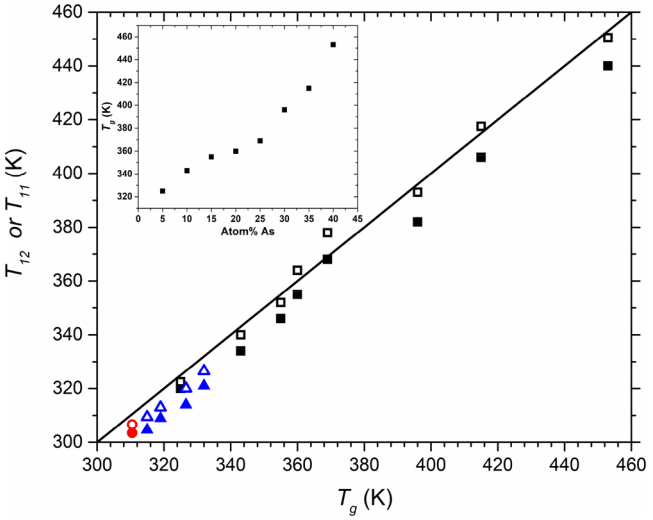

Figure 2. T_{12} (solid symbol) and T_{11} (open symbols) for Se (red circles), As−Se (black squares) and Se−Te (blue triangles) liquids obtained from viscosity data reported in ref 10 as a function of T_g determined by DSC in the present study and reported in ref 22. T_g = T_{12} or T_{11} is denoted by solid line. Inset shows the compositional dependence of T_g of all As−Se glasses determined in this study (see Table 1).

equation.[11−14] Similar variation can also be found in the literature for another relatively fragile liquid $As_{10}Se_{90}$ where the experimentally determined m ranges between ∼35 and 68.[15−18] On the other hand, the assumption of $\eta \approx 10^{12}$ Pa s at $T \approx T_g$ may not be tenable for all glass-forming liquids, which may lead to further discrepancy in the estimation of m. In fact it is well-known that, unlike oxide liquids,[19] chalcogenide glass-forming liquids almost universally display a viscosity that is significantly lower than 10^{12} Pa s at $T \approx T_g$.[20−22] This difference between T_g and T_{12}, the temperature where the measured viscosity is indeed 10^{12} Pa s (Figure 2), results mostly from the fact that the glassy shear modulus G_∞ of chalcogenide liquids (3−5 GPa) is nearly 1 order of magnitude lower than that characteristic of oxides (∼30 GPa). The shear relaxation time τ_{shear} is related to viscosity via the Maxwell relation: $\tau_{shear} = \eta/G_\infty$. Considering τ_{shear} to be equal to the enthalpy relaxation time $\tau_{en} \approx 100$ s at T_g, when T_g is determined by differential scanning calorimetry (DSC) using a typical heating/cooling rate of 10 K/s, one obtains $\eta = G_\infty \tau_{shear}$ to be $\sim 10^{12.5}$ Pa s for oxides and $\sim 10^{11.5}$ for chalcogenides. Therefore, m obtained from a η vs T_g/T curve may be underestimated if $T_g > T_{12}$. Fortunately, the effect of this inequality between T_g and T_{12} on m in most cases is relatively small and can be resolved if T_g in eq 1 is replaced by T_{12}. However, it may be noted here that these estimations are based on the implicit assumption that $\tau_{shear} = \tau_{en}$, which may not always hold true, especially for highly fragile liquids (see below).

Alternatively, m in eq 1 can be expressed as a function of the activation energy of shear relaxation E measured at $T \approx T_g$

$$m = \frac{E}{RT_g \ln 10} \tag{2}$$

Such a relationship between E and m enables the use of DSC to measure m under the assumption that shear relaxation measured by viscometry and enthalpy relaxation measured by DSC have the same activation energy. In the case of DSC experiments performed at different heating/cooling rates q, the dependence of the fictive temperature T_f on q yields this activation energy Δh for enthalpy relaxation according to the relation:

$$\frac{\mathrm{d} \ln q}{\mathrm{d}\left(\frac{1}{T_f}\right)} = -\frac{\Delta h}{R} \tag{3}$$

Here, T_f can be defined as the temperature where, upon cooling, a supercooled liquid falls out of equilibrium and the structure of the liquid is frozen in as it enters the glassy state. Setting $\Delta h = E$ in eq 3 can then yield m from eq 2. Therefore, considering the experimental challenges associated with direct viscosity determination at or near T_g, DSC appears to be a good substitute technique for the determination of m, provided Δh is indeed equal to E. However, Zheng et al. recently determined m for a wide variety of borate, aluminosilicate and tellurite glass-forming liquids from independent measurements of Δh and E, and reported a significant discrepancy between their kinetic fragility indices determined from E and calorimetric fragility indices determined from Δh.[23] The kinetic fragility was shown to be consistently higher than the calorimetric fragility for these liquids. This discrepancy was attributed by the authors to the Arrhenius approximation of the relation shown in eq 3 in the glass transition range, while the kinetic fragility was clearly non-Arrhenius. In contrast, Schawe[24] demonstrated the validity of the Frenkel-Kobeko-Reiner (FKR) relation: $q\tau_{shear}$ = constant for fragile liquid polystyrene. It may be noted that since $\tau_{shear} = \eta/G_\infty$ and G_∞, being weakly temperature dependent, can be treated as a temperature-independent constant for a specific glass-former, the FKR relation also suggests that $q\eta$ = constant. Therefore, Schawe's observation questions the validity of the argument put forward by Zheng et al. that the Arrhenius approximation in eq 3 is the source of the discrepancy between Δh and E.[23,24]

https://dx.doi.org/10.1021/acs.jpcb.0c11278
J. Phys. Chem. B XXXX, XXX, XXX−XXX

Here we further explore these issues in a systematic study of the determination of m of As_xSe_{100-x} ($0 \le x \le 40$) liquids using both kinetic and calorimetric methods. The viscosity of these liquids is determined near the glass transition region using both parallel-plate rheometry and beam bending viscometry, while the heating rate dependence of the fictive temperature is measured using conventional DSC measurements. Additionally, for select compositions, modulated DSC (MDSC) measurements are employed to obtain τ_{en}, which is then compared to the shear relaxation time to examine the validity of the assumption $\tau_{shear} = \tau_{en}$.

2. EXPERIMENTAL SECTION

2.1. Sample Synthesis and Calorimetric Characterization. The As_xSe_{100-x} ($0 \le x \le 40$) glasses were prepared in 10 g batches from the constituent elements (≥99.999% purity, metal basis) by the conventional melt-quenching method. The mixture of constituent elements was loaded into a fused quartz ampule that was evacuated to 10^{-4} Torr. The batches were melted at 650 °C for at least 24 h in a rocking furnace. The melts were subsequently quenched by dipping the ampule in water. The synthesis of the Te_5Se_{95} glass was reported in a previous study[22] and the same samples are used in the present study. As_xSe_{100-x} glass rods with a square cross-section for the purpose of measuring viscosity using the beam bending technique were made by melting appropriate mixtures of As and Se using ampules in which the lowest 15 cm length was fabricated from square fused quartz tubing with internal dimensions of 4 × 4 mm. After quenching the melt to glass by dipping the ampule in water, the selenide glass rods were extracted by etching off the overlying fused quartz sleeving with HF, yielding bars with a typical length of 10 cm.

The T_g of the as-made glasses was determined using DSC (Mettler Toledo DSC1). Samples of mass ∼10−25 mg were hermetically sealed in aluminum pans. The T_f was taken as the onset of the endothermic glass transition signal while heating the sample at a specific rate q K/s, following cooling at the same rate from T_g + 30 K to T_g − 50 K. In the case of modulated DSC (MDSC) experiments, a thin sample piece of mass ∼5−10 mg was heated to T_g + 50 K, isothermally held for 1 min to erase the thermal history, and subsequently cooled to T_g − 50 K at a constant rate of 2 K/min. After equilibrating for 5 min, the sample was reheated from this temperature to T_g + 30 K at an average heating rate of 2 K/min with a sinusoidal modulation superimposed onto the conventional linear heating rate ramp. The modulation amplitude was set to 1 K and the modulation period was 120 s. The out of phase, imaginary component of complex heat capacity C_p^* can be calculated according to $C_p'' = |C_p^*| \sin\theta$, where θ is the phase angle between the sinusoidal modulated heat flow signal and the modulated heating rate.[25] The instrumental phase lag was compensated to obtain a flat baseline for C_p''.

2.2. Viscosity Measurement. The shear viscosity in the range of ∼10^8−10^{12} Pa s of the supercooled As_xSe_{100-x} liquids was measured using a parallel plate rheometer (MCR302, Anton Paar, U.S.A.) in a flowing nitrogen environment. The sample was first rapidly heated up to a softening temperature and then pressed and trimmed into a sandwich-like geometry with a thickness of ∼1 mm. After reaching thermal equilibrium at the desired measurement temperature, a constant shear stress τ was applied to the sample while the strain response was recorded as a function of time. After reaching a steady state the strain rate $\dot{\gamma}$ no longer changes with time, corresponding to a linear viscous response. The viscosity is subsequently obtained from the relation: $\eta = \frac{\tau}{\dot{\gamma}}$ (Figure 3). Shear viscosity in the range

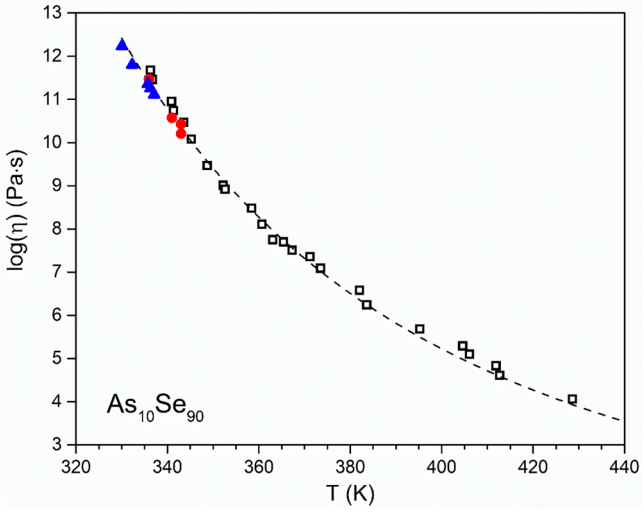

Figure 3. Comparison between viscosity of $As_{10}Se_{90}$ liquids reported in ref 16 (black squares) and determined in the present study in the high viscosity range using parallel-plate rheometry (red circles) and beam bending method (blue triangles). Dashed line through the data points is a guide to the eye.

∼10^{11}−$10^{12.5}$ Pa·s was measured for select As_xSe_{100-x} liquids (x = 0, 10, 20 and 30) using the beam bending method (Figure 3). Three-point beam bending viscosity measurements were made by utilizing a custom-design beam bending setup. The measurements were carried out on an alumina stage using 4 mm × 4 mm beams. The span size of the alumina stage was 56 mm and a constant force of 46g was applied for all the measurements. The deflection was measured using a linear variable differential transformer (LVDT). The calibration of the LVDT and the temperature was checked with low temperature internal standard materials as well as standard viscosity reference glasses (710, 710A, and 717A) from the National Institute of Standards and Technology (NIST). The instantaneous viscosity was calculated using the equation:[26]

$$\eta = \frac{gL^3}{1440 I_c (dh/dt)}\left[M + \frac{\rho AL}{1.6}\right] \quad (4)$$

where η is the viscosity, L is the span size, M is the applied load, g is the acceleration of gravity, ρ is the density of the glass, A is the cross-sectional area, h is the deflection measured by LVDT, t is the time, and I_c is the cross-section moment of inertia of the beam. Each sample was heated to an initial temperature that corresponds to approximately $10^{10.5}$ Pa s and held isothermally about 2 min to help erase the thermal history. Then they were cooled to the target viscosity in the vicinity of the glass transition at a rate of 2 K/min and isothermally held until the viscosity became time independent. The thermodynamic and the thermal equilibrium state were confirmed by the linear deflection of the beam with time which corresponds to a constant equilibrium viscosity. The viscosity values from both parallel plate and beam bending methods are found to be in good agreement with the data reported in the literature obtained using different techniques (Figure 3).

https://dx.doi.org/10.1021/acs.jpcb.0c11278
J. Phys. Chem. B XXXX, XXX, XXX−XXX

Table 1. Fragility Indices m_{vis} and m_{DSC} Determined from Viscosity and Calorimetry Measurements, Respectively, T_{12} and T_g for As−Se Liquids[a]

composition x	m_{vis}^{PP}	m_{vis}^{BB}	m_{DSC}	T_{12} (K)	T_g (K)
0	83.0 ± 3.0	86.6 ± 0.6	81.0 ± 3.0	304	311
5	72.8 ± 5.4	not measured	71.8 ± 3.2	320	325
10	60.3 ± 3.0	51.0 ± 2.3	56.7 ± 3.5	334	343
15	39.5 ± 4.3	not measured	36.9 ± 3.0	346	355
20	31.2 ± 2.5	37.9 ± 0.5	31.9 ± 2.0	355	360
25	30.6 ± 1.6	not measured	30.0 ± 2.0	368	369
30	33.1 ± 0.3	32.1 ± 0.2	32.3 ± 1.3	382	396
35	35.5 ± 3.1	not measured	31.0 ± 2.6	406	415
38	not measured	not measured	34.9 ± 1.0	not measured	439
40	37.8 ± 1.7	not measured	41.3 ± 1.6	440	453

[a]Superscripts PP and BB denote viscosity data from parallel plate and beam bending measurements, respectively.

3. RESULTS AND DISCUSSION

3.1. Kinetic Fragility. The activation energy of viscous flow E for all As_xSe_{100-x} liquids studied here is obtained from the slope of ln η vs $1000/T$ using parallel-plate viscosity data in the range $\sim 10^{10}-10^{12}$ Pa s and beam-bending viscosity data in the range $\sim 10^{11}-10^{12.5}$ Pa s. The kinetic fragility m_{vis} is subsequently obtained from E using eq 2 and is listed in Table 1 as well as shown in Figure 4. The m_{vis} values estimated from

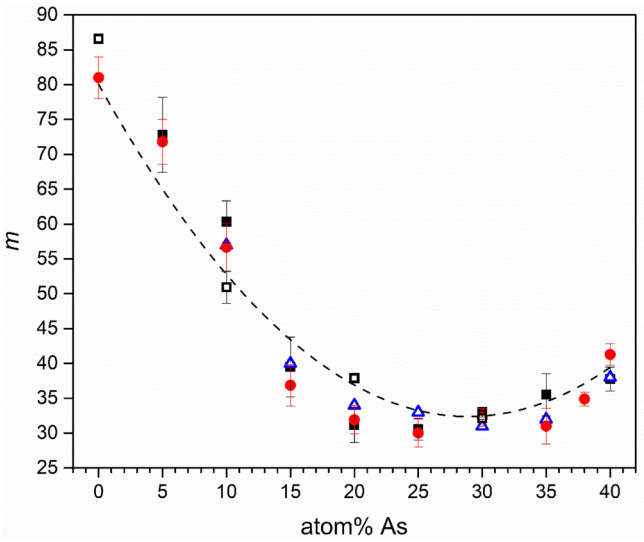

Figure 4. Comparison between kinetic fragility indices determined using parallel-plate rheometry (solid black squares) and beam bending method (open black squares), and calorimetric (red circles) fragility indices m for the As_xSe_{100-x} system, determined in the present study. Kinetic fragility indices reported by Yang et al.[18] (blue open triangles) are shown for comparison. Dashed curve through the data points is a guide to the eye only.

the parallel-plate and the beam-bending viscosity data display good agreement, within the limits of experimental error (Table 1 and Figure 4). The fragility index m_{vis} drops with increasing As content precipitously from ~83 for pure Se to a broad minimum value of ~31 in the interval $20 \leq x \leq 30$, followed by a slight rise to ~38 between $35 \leq x \leq 40$. Previous studies have shown that the high m value of pure Se reflects the large conformational entropy available to the relatively long disjointed chains of two-coordinated Se atoms that constitute this liquid. Progressive cross-linking of these chains with 3-coordinated As atoms results in a rapid shortening of the length L of these Se chain segments and a concomitant drop in their conformational entropy.[27] Rheological studies in the literature demonstrate that, as L approaches ~3 to 4 near the composition $As_{20}Se_{80}$, these short selenium chain segments cannot generate significant entropy via conformation change and the network becomes rigid.[28] Within the framework of the chain-crossing model further addition of As would result in continued shortening of these Se chain segments and ultimately a three-dimensionally connected network of corner-shared $AsSe_{3/2}$ pyramids would emerge at the stoichiometric composition of $As_{40}Se_{60}$. Therefore, the conformational entropy would continually decrease with increasing As content beyond 20 atom %, albeit at a significantly slower rate, consistent with the plateau in m in the interval $20 \leq x \leq 30$. Therefore, in this scenario the rise in m between $35 \leq x \leq 40$ may appear to be anomalous. A number of studies in the literature have claimed this apparent anomaly to be a signature of the presence of the so-called "Boolchand intermediate phase" in the composition interval where m goes through a broad minimum and a manifestation of an optimally constrained network.[29,30] According to this hypothesis the rise in m for $x \geq 35$ signals an increasingly overconstrained network. However, the structural origin of the intermediate phase remains debatable in the literature.[31] On the other hand, a natural explanation of the rise in m between $35 \leq x \leq 40$ in Figure 4 can be sought in the configurational entropic explanation of fragility. Recent isotope-substituted neutron diffraction and high-resolution ^{77}Se nuclear magnetic resonance spectroscopic studies have conclusively shown a significant violation of chemical order and the presence of homopolar Se−Se and therefore As−As bonds even in the nominally stoichiometric $As_{40}Se_{60}$ glass.[32,33] Such violation of chemical order allows for temperature driven structural speciation reactions such as $2\,[\text{As}-\text{Se}] \xrightarrow{T} [\text{Se}-\text{Se}] + [\text{As}-\text{As}]$, which can generate configurational entropy in the liquid with increasing temperature.

3.2. Calorimetric Fragility. The T_f of the As_xSe_{100-x} glasses was determined as a function of the cooling rate q varying over more than 2 orders of magnitude, following the method of Wei et al. and m was subsequently determined using eq 3 in the temperature region near T_{12}. These m values are compared in Table 1 and in Figure 4 with those obtained from viscosity. It is clear that the kinetic and calorimetric m values display good agreement for all compositions. A comparison between the temperature dependence of q and $1/\tau_{shear} = \frac{G_\infty}{\eta}$ is shown for a relatively strong liquid $As_{30}Se_{70}$ ($m \approx 33$) and for the fragile

https://dx.doi.org/10.1021/acs.jpcb.0c11278
J. Phys. Chem. B XXXX, XXX, XXX−XXX

liquid Se ($m \approx 80$) in an Arrhenius-type plot (Figure 5). It is to be noted that here G_∞ was taken as a temperature-independent

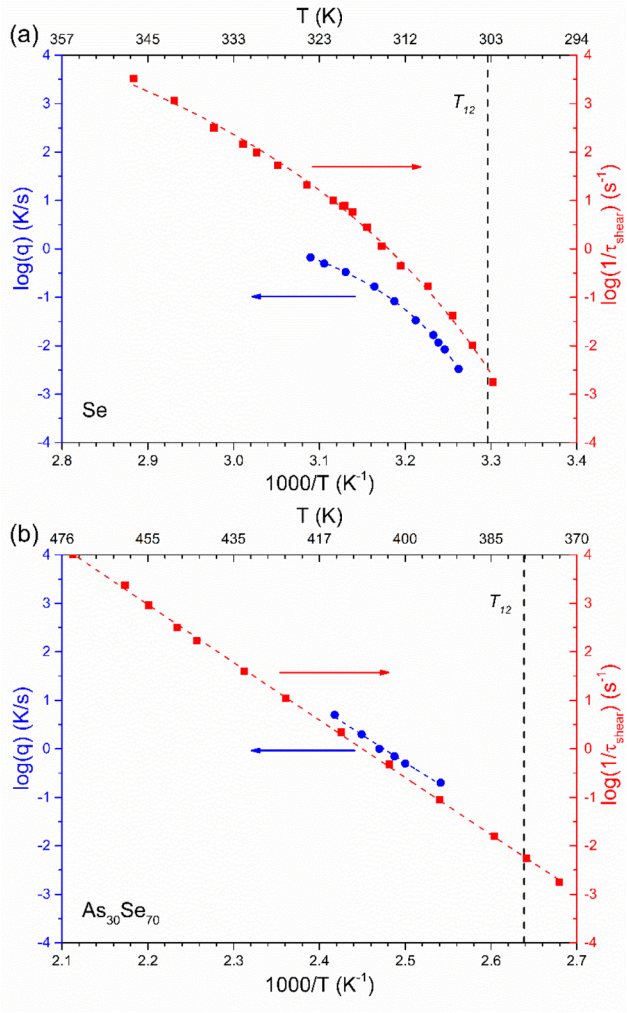

Figure 5. Heating rate vs fictive temperature (left ordinate, blue circles) determined in the present study and of the shear relaxation rate (right ordinate, red squares) for (a) Se and (b) $As_{30}Se_{70}$ liquids. The shear relaxation rates are calculated from viscosity data reported in the literature[9,16] using the Maxwell relation, where the temperature-independent G_∞ is taken to be 3.2 and 6 GPa, for Se and $As_{30}Se_{70}$, respectively.[39] The dashed curves are least-squares fits of the VFT equation to these data sets. T_{12} is denoted by black dashed vertical lines.

constant for the estimation of $1/\tau_{shear}$, which may not be strictly valid for $T > T_g$.[34] The close correspondence between the temperature variations of q and $1/\tau_{shear}$ is consistent with past observations[24,35] on organic and inorganic oxide network glass-forming liquids and indicates the validity of the FKR relation. The pronounced non-Arrhenius temperature variation of both q and $1/\tau_{shear}$ in the fragile liquids, accompanied by a significant offset between their isothermal values by a nearly constant factor (Figure 5), underscores the importance of using identical ranges of q and $1/\tau_{shear}$ in obtaining consistent m values from viscosity and calorimetry. The observation in Figure 5 that $q \ll 1/\tau_{shear}$ in highly fragile liquids such as Se indicates that the assumption $\tau_{shear} = \tau_{en}$ under isothermal conditions may not be tenable and $\tau_{en} \gg \tau_{shear}$. Since $\tau_{en} \approx 100$ s at T_g determined by DSC using typical heating/cooling rates of ~10 K/min and $\tau_{shear} \approx 100$s at T_{12}, T_g must be located above T_{12} in these fragile liquids. In fact, the discrepancy between real viscosity at T_g and the expected viscosity of $10^{11.5\pm0.5}$ Pa s rapidly increases with increasing m in highly fragile chalcogenide liquids (Figure 6). For an offset between q

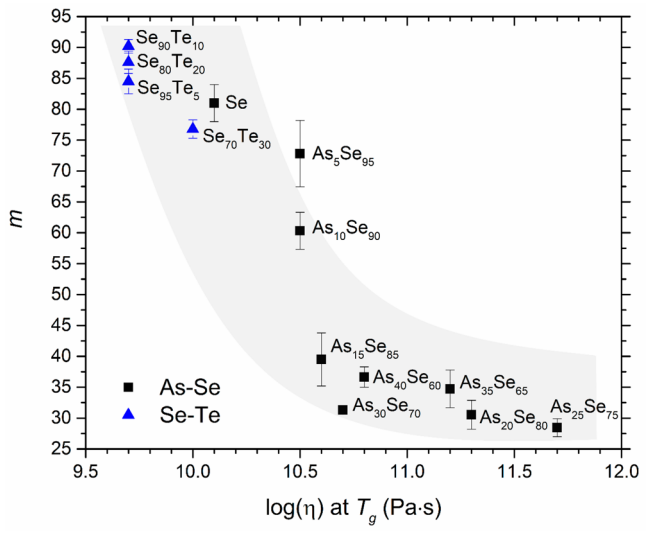

Figure 6. Kinetic fragility index m of As−Se (black squares) and Se−Te[10] (blue triangles) liquids as a function of viscosity at T_g determined from DSC heating scans at a rate of 10 K/min.

and $1/\tau_{shear}$ by a nearly constant factor with $q \ll 1/\tau_{shear}$, this will lead to a kinetic fragility index that is consistently higher than the calorimetric fragility when the viscosity data for a fragile liquid near T_g are either limited or not available (e.g., in the case of many metallic glass-forming liquids[36]) and T_g is implicitly assumed to be identical to T_{12} (Figure 5). As noted above, such an inconsistency between the kinetic and calorimetric m was indeed reported by Zheng et al. in a previous study.[23] Consequently, for Se one needs to compare the activation energy for viscosity near T_{12} with that of enthalpy relaxation at $q \approx 10^{-2}$ K/s to obtain a consistent m value by both methods (Figure 5).

3.3. Enthalpy vs Shear relaxation. The hypothesis that $\tau_{en} \neq \tau_{shear}$ for highly fragile glass-forming liquids is further explored in a fragile $Se_{95}Te_5$ ($m \approx 85$) and a strong $As_{25}Se_{75}$ ($m \approx 28$) chalcogenide liquid where τ_{en} is directly determined using MDSC experiments. The C_p'' maximum corresponding to the temperature oscillation period $P = 120$ s in the MDSC experiments provides the characteristic time scale for $\tau_{en} \approx P/2\pi = 19$ s.[18] This τ_{en} value is compared to τ_{shear} at the same temperature in Figure 7, where the latter was obtained from the experimental η, using the Maxwell relation $\tau_{shear} = \eta/G_\infty$. It is clear from Figure 7 that, while $\tau_{en} \approx 3.8*\tau_{shear}$ for the strong $As_{25}Se_{75}$ liquid, $\tau_{en} \approx 19.8*\tau_{shear}$ for the fragile $Se_{95}Te_5$ liquid. The latter result is indeed consistent with the observation of $q \ll 1/\tau_{shear}$ for liquid Se (Figure 5). Liquids with high fragility indices are known to be characterized by rather wide distributions of the relaxation times near T_g and the observation of $\tau_{en} \neq \tau_{shear}$ suggests that enthalpy and shear relaxation sample different parts of this distribution.[23,37] Strong temporal decoupling between enthalpy and shear relaxation time scales has also been reported for fragile TeO_2-based oxide glass-forming liquids by Komatsu et al.[38] where the authors ascribed the decoupling to structural and dynamical hetero-

https://dx.doi.org/10.1021/acs.jpcb.0c11278
J. Phys. Chem. B XXXX, XXX, XXX−XXX

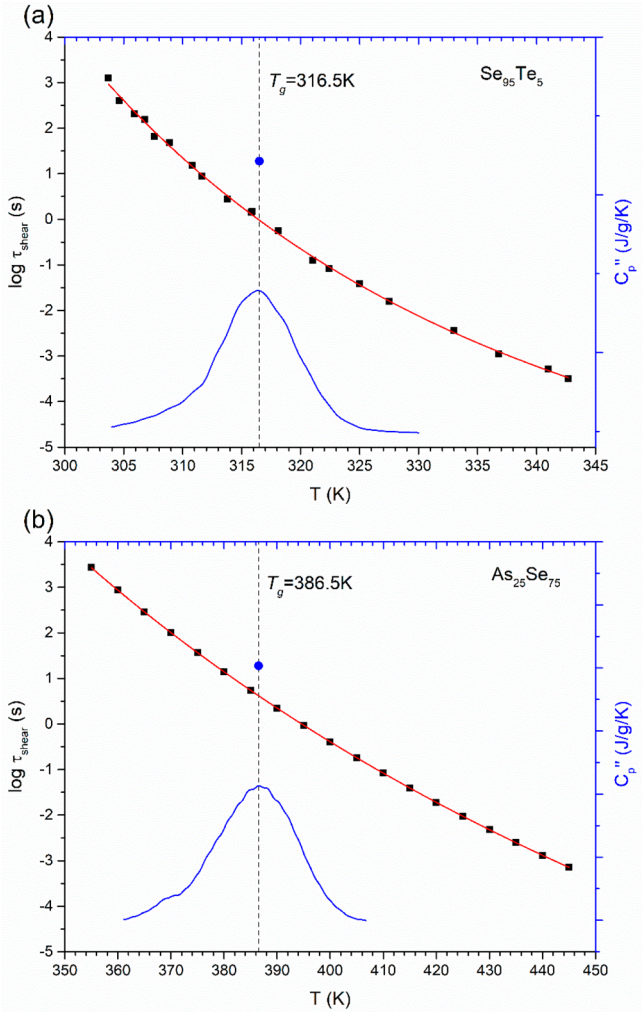

Figure 7. Temperature dependence of τ_{shear} (left ordinate) and C_P'' collected with a modulating period P = 120 s and a heating rate of 10 K/min (right ordinate) for (a) $Se_{95}Te_5$ and (b) $As_{25}Se_{75}$. Solid lines through the viscosity data correspond to least-squares fits to the MYEGA equation. The blue circles represent $\tau_{en} \approx P/2\pi$ = 19 s at the peak temperature of C_P''.

geneities that are characteristic of fragile liquids. In this scenario deeply supercooled fragile liquids are characterized by highly constrained or strongly bonded regions that are characterized by slow, cooperative dynamics and these regions are surrounded and connected via weakly constrained regions that perform fast dynamics. For example, for pure Se and Se-rich fragile As−Se liquids investigated in the present study, these strongly vs weakly constrained regions likely correspond, respectively, to regions of high and low degrees of Se chain entanglement and/or cross-linking density. Motion in the weakly constrained regions can dynamically percolate and control viscous flow and shear relaxation. In contrast, enthalpy relaxation would require a global structural rearrangement involving both strongly constrained regions with slow dynamics and weakly constrained regions with fast dynamics. Consequently, τ_{en} can be significantly larger than τ_{shear} in fragile liquids with strong dynamical heterogeneity. However, this hypothesis is yet to be experimentally validated, and moreover it remains to be seen whether $\tau_{en} \gg \tau_{shear}$ is generally valid for all classes of fragile glass-forming liquids in the deeply supercooled regime.

4. CONCLUSION

Despite the simplicity of its definition, the determination of m using the temperature dependence of shear vs enthalpy relaxation may lead to inconsistent results, especially in the case of highly fragile liquids. Results from conventional DSC and MDSC measurements indicate that, although the activation energies for the enthalpy and shear relaxation in these liquids near their glass transition are similar, τ_{en} can be slower than τ_{shear} by more than 1 order of magnitude. This discrepancy between τ_{en} and τ_{shear} along with the assumption $T_g \approx T_{12}$ may lead to a consistently higher value of kinetic m, compared to the calorimetric m for highly fragile liquids.

AUTHOR INFORMATION

Corresponding Author

Sabyasachi Sen − *Department of Materials Science & Engineering, University of California at Davis, Davis, California 95616, United States;* orcid.org/0000-0002-4504-3632; Email: sbsen@ucdavis.edu

Authors

Yiqing Xia − *Department of Materials Science & Engineering, University of California at Davis, Davis, California 95616, United States*

Bing Yuan − *Department of Materials Science & Engineering, University of California at Davis, Davis, California 95616, United States*

Ozgur Gulbiten − *Science & Technology Division, Corning Inc., Corning, New York 14831, United States;* orcid.org/0000-0001-9156-7659

Bruce Aitken − *Science & Technology Division, Corning Inc., Corning, New York 14831, United States*

Complete contact information is available at: https://pubs.acs.org/10.1021/acs.jpcb.0c11278

Notes

The authors declare no competing financial interest.

ACKNOWLEDGMENTS

This study was supported by the National Science Foundation Grant NSF-DMR 1855176. The authors wish to thank David Walmsley for his contributions to the calibration of the beam bending viscosity measurements in the vicinity of the glass transition, Dan Frank for the fabrication of the specialized ampules used for making square cross-section glass rods, and Jason Brown for his assistance with glass synthesis.

REFERENCES

(1) Rawson, H. Physics of Glass Manufacturing Processes. *Phys. Technol.* **1974**, *5* (2), 91−114.

(2) Lian, Z. G.; Pan, W.; Furniss, D.; Benson, T. M.; Seddon, A. B.; Kohoutek, T.; Orava, J.; Wagner, T. Embossing of Chalcogenide Glasses: Monomode Rib Optical Waveguides in Evaporated Thin Films. *Opt. Lett.* **2009**, *34* (8), 1234−1236.

(3) Savage, S. D.; Miller, C. A.; Furniss, D.; Seddon, A. B. Extrusion of Chalcogenide Glass Preforms and Drawing to Multimode Optical Fibers. *J. Non-Cryst. Solids* **2008**, *354* (29), 3418−3427.

(4) Zhang, X. H.; Guimond, Y.; Bellec, Y. Production of Complex Chalcogenide Glass Optics by Molding for Thermal Imaging. *J. Non-Cryst. Solids* **2003**, *326*−*327*, 519−523.

(5) Novikov, V. N.; Ding, Y.; Sokolov, A. P. Correlation of Fragility of Supercooled Liquids with Elastic Properties of Glasses. *Phys. Rev. E* **2005**, *71* (6), 061501.

https://dx.doi.org/10.1021/acs.jpcb.0c11278
J. Phys. Chem. B XXXX, XXX, XXX−XXX

(6) Angell, C. A. Perspective On the Glass Transition. *J. Phys. Chem. Solids* **1988**, *49*, 863−871.
(7) Angell, C. A. Relaxation in Liquids, Polymers and Plastic Crystals - Strong/Fragile Patterns and Problems. *J. Non-Cryst. Solids* **1991**, *131*, 13−31.
(8) Böhmer, R.; Angell, C. A. Local and Global Relaxations in Glass Forming Materials. In *Disorder effects on relaxational processes*; Richert, R., Blumen, A., Eds.; Springer: Berlin, Heidelberg, 1994; pp 11−54.
(9) Koštál, P.; Málek, J. Viscosity of Selenium Melt. *J. Non-Cryst. Solids* **2010**, *356*, 2803−2806.
(10) Koštál, P.; Málek, J. Viscosity of Se-Te Glass-Forming System. *Pure Appl. Chem.* **2015**, *87* (3), 239−247.
(11) Fulcher, G. S. Analysis of Recent Measurements of the Viscosity of Glasses. *J. Am. Ceram. Soc.* **1925**, *8* (6), 339−355.
(12) Tammann, G. H. W. Z.; Hesse, W. The Dependence of Viscosity upon the Temperature of Supercooled Liquids. *Z. Anorg. Allg. Chem.* **1926**, *156*, 245−257.
(13) Mauro, J. C.; Yue, Y.; Ellison, A. J.; Gupta, P. K.; Allan, D. C. Viscosity of Glass-Forming Liquids. *Proc. Natl. Acad. Sci. U. S. A.* **2009**, *106*, 19780−19784.
(14) Avramov, I.; Milchev, A. Effect of Disorder on Diffusion and Viscosity in Condensed Systems. *J. Non-Cryst. Solids* **1988**, *104*, 253−260.
(15) Nemilov, S. V.; Petrovskii, G. T. A Study of the Viscosity of Selenium-Arsenic Glasses. *Zn. Prikl. Khim* **1963**, *36*, 977−981.
(16) Bernatz, K. M.; Echeverría, I.; Simon, S. L.; Plazek, D. J. Characterization of the Molecular Structure of Amorphous Selenium Using Recoverable Creep Compliance Measurements. *J. Non-Cryst. Solids* **2002**, *307*, 790−801.
(17) Musgraves, J. D.; Wachtel, P.; Novak, S.; Wilkinson, J.; Richardson, K. Composition Dependence of the Viscosity and Other Physical Properties in the Arsenic Selenide Glass System. *J. Appl. Phys.* **2011**, *110*, 063503.
(18) Yang, G.; Gulbiten, O.; Gueguen, Y.; Bureau, B.; Sangleboeuf, J.-C.; Roiland, C.; King, E. A.; Lucas, P. Fragile-Strong Behavior in the As_xSe_{1-x} Glass Forming System in Relation to Structural Dimensionality. *Phys. Rev. B: Condens. Matter Mater. Phys.* **2012**, *85*, 144107.
(19) Yue, Y. The Iso-Structural Viscosity, Configurational Entropy and Fragility of Oxide Liquids. *J. Non-Cryst. Solids* **2009**, *355* (10−12), 737−744.
(20) Pustková, P.; Shánelová, J.; Málek, J.; Cicmanec, P. Relaxation Behavior of Selenium Based Glasses. *J. Therm. Anal. Calorim.* **2005**, *80*, 643−647.
(21) Koštál, P.; Shánelová, J.; Málek, J. Viscosity of Chalcogenide Glass-Formers. *Int. Mater. Rev.* **2020**, *65* (2), 63−101.
(22) Yuan, B.; Aitken, B.; Sen, S. Rheology of Supercooled Se-Te Chain Liquids: Role of Te as an Interchain Cross-Linker. *J. Non-Cryst. Solids* **2020**, *529*, 119764.
(23) Zheng, Q.; Mauro, J. C.; Yue, Y. Reconciling Calorimetric and Kinetic Fragilities of Glass-Forming Liquids. *J. Non-Cryst. Solids* **2017**, *456*, 95−100.
(24) Schawe, J. E. K. Vitrification in a Wide Cooling Rate Range: The Relations between Cooling Rate, Relaxation Time, Transition Width, and Fragility. *J. Chem. Phys.* **2014**, *141*, 184905.
(25) Gulbiten, O.; Mauro, J. C.; Lucas, P. Relaxation of Enthalpy Fluctuations during Sub-Tg Annealing of Glassy Selenium. *J. Chem. Phys.* **2013**, *138*, 244504.
(26) ASTM C 1350M-96 *Standard Test Method for Measurement of Viscosity of Glass between Softening Point and Annealing Range (Approximately 10^8 Pa·s to Approximately 10^{13} Pa·s) by Beam Bending (Metric)*; American Society for Testing and Materials: West Conshohocken, PA, 2019.
(27) Zhu, W.; Aitken, B.; Sen, S. Investigation of the Shear Relaxation Behavior of As-Se Liquids within the Framework of Entropic and Elastic Models of Viscous Flow. *J. Non-Cryst. Solids* **2020**, *534*, 119959.
(28) Sen, S.; Xia, Y.; Zhu, W.; Lockhart, M.; Aitken, B. Nature of the Floppy-to-Rigid Transition in Chalcogenide Glass-Forming Liquids. *J. Chem. Phys.* **2019**, *150*, 144509.
(29) Bauchy, M.; Micoulaut, M.; Boero, M.; Massobrio, C. Compositional Thresholds and Anomalies in Connection with Stiffness Transitions in Network Glasses. *Phys. Rev. Lett.* **2013**, *110*, 165501.
(30) Ravindren, S.; Gunasekera, K.; Tucker, Z.; Diebold, A.; Boolchand, P.; Micoulaut, M. Crucial Effect of Melt Homogenization on the Fragility of Non-Stoichiometric Chalcogenides. *J. Chem. Phys.* **2014**, *140*, 134501.
(31) Zeidler, A.; Salmon, P. S.; Whittaker, D. A. J.; Pizzey, K. J.; Hannon, A. C. Topological Ordering and Viscosity in the Glass-Forming Ge-Se System: The Search for a Structural or Dynamical Signature of the Intermediate Phase. *Front. Mater.* **2017**, *4*, 32.
(32) Polidori, A.; Zeidler, A.; Salmon, P. S. Structure of As-Se Glasses by Neutron Diffraction with Isotope Substitution. *J. Chem. Phys.* **2020**, *153*, 154507.
(33) Kaseman, D. C.; Hung, I.; Gan, Z.; Aitken, B.; Currie, S.; Sen, S. Structural and Topological Control on Physical Properties of Arsenic Selenide Glasses. *J. Phys. Chem. B* **2014**, *118*, 2284−2293.
(34) Gueguen, Y.; Rouxel, T.; Gadaud, P.; Bernard, C.; Keryvin, V.; Sangleboeuf, J. C. High-Temperature Elasticity and Viscosity of Ge_xSe_{1-x} Glasses in the Transition Range. *Phys. Rev. B: Condens. Matter Mater. Phys.* **2011**, *84*, 064201.
(35) Yue, Y.; Von der Ohe, R.; Jensen, S. L. Fictive Temperature, Cooling Rate, and Viscosity of Glasses. *J. Chem. Phys.* **2004**, *120* (17), 8053−8059.
(36) Zhang, C.; Hu, L.; Yue, Y.; Mauro, J. C. Fragile-to-Strong Transition in Metallic Glass-Forming Liquids. *J. Chem. Phys.* **2010**, *133*, 014508.
(37) Potuzak, M.; Welch, R. C.; Mauro, J. C. Topological Origin of Stretched Exponential Relaxation in Glass. *J. Chem. Phys.* **2011**, *135*, 214502.
(38) Komatsu, T.; Aida, K.; Honma, T.; Benino, Y.; Sato, R. Decoupling between Enthalpy Relaxation and Viscous Flow and Its Structural Origin in Fragile Oxide Glass-Forming Liquids. *J. Am. Ceram. Soc.* **2002**, *85* (1), 193−199.
(39) Yang, G.; Bureau, B.; Rouxel, T.; Gueguen, Y.; Gulbiten, O.; Roiland, C.; Soignard, E.; Yarger, J. L.; Troles, J.; Sangleboeuf, J. C.; et al. Correlation between Structure and Physical Properties of Chalcogenide Glasses in the As_xSe_{1-x} System. *Phys. Rev. B: Condens. Matter Mater. Phys.* **2010**, *82*, 195206.

https://dx.doi.org/10.1021/acs.jpcb.0c11278
J. Phys. Chem. B XXXX, XXX, XXX−XXX